Volume 28
Number 4
26 January 2026
Pages 1843-2124

Green Chemistry

Cutting-edge research for a greener sustainable future

rsc.li/greenchem

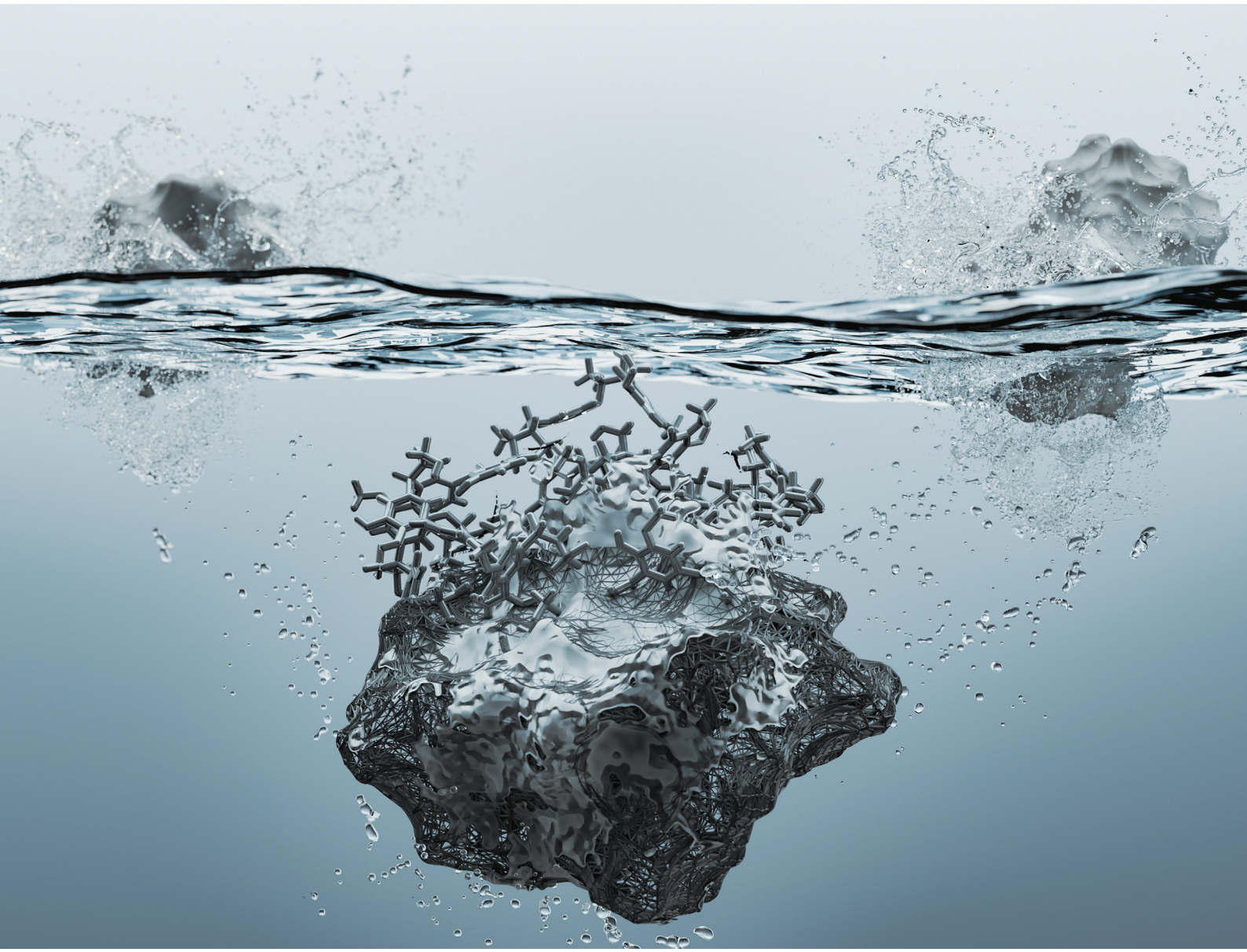

ISSN 1463-9262

ROYAL SOCIETY OF CHEMISTRY

PAPER

Orlando J. Rojas, Kwang Ho Kim *et al.*
Hydrophobic and mechanically reinforcing coatings from palmitoylated lignin *via* waterborne spraying

Green Chemistry

PAPER

View Article Online
View Journal | View Issue

Cite this: *Green Chem.*, 2026, **28**, 1924

Hydrophobic and mechanically reinforcing coatings from palmitoylated lignin *via* waterborne spraying

Jie Wu, †[a,b,c] Nathan Huang,†[b] Daniel Barker-Rothschild, [a,c] Zhangmin Wan, [a,c] Minke Yang,[a,b] Xin Shu, [a,c] Yi Hu, [a] Joshua Booth, [d] Oliver Evenden, [d] Orlando J. Rojas *[a,b,c,e] and Kwang Ho Kim *[a,b]

Softwood Kraft lignin was esterified with palmitic anhydride to produce palmitoylated lignin (p-lignin). Structural analyses by FTIR and quantitative ^{31}P NMR confirmed high degrees of hydroxyl substitution (71% aliphatic and 82% phenolic). Thermal measurements revealed marked plasticization, with the glass transition temperature shifting from 170 °C to 61 °C. The p-lignin resulting from the modification was more hydrophobic, as confirmed by reduced dynamic vapor sorption and molecular dynamics simulations showing lower hydration free energy and significantly stronger binding free energy. When applied from acetone solution onto paper, p-lignin produced coatings with water contact angles (WCA, 1 min) exceeding 150°, although low-temperature curing (80 °C) was required to achieve adequate adhesion. In contrast, waterborne colloidal suspensions of p-lignin particles, prepared *via* solvent-shift and stabilized with hydroxyethyl cellulose (HEC), could be sprayed directly onto paper to yield uniform coatings with WCA values above 130° (1 min) and strong adhesion, without any need for post-treatment. The coatings greatly enhanced filter paper's mechanical performance, with dry and wet tensile strength increasing by 65% and 400%, respectively. Using palmitic groups (C16) as a model, we show that grafting long hydrocarbon chains onto lignin imparts durable hydrophobicity and mechanical reinforcement, highlighting palmitoylated lignin as a promising bio-based coating for sustainable applications.

Received 12th October 2025,
Accepted 11th November 2025

DOI: 10.1039/d5gc05423k

rsc.li/greenchem

Green foundation

1. This work establishes a new paradigm for lignin valorization by demonstrating a solvent-minimized, waterborne route to create multifunctional coatings. It integrates molecular-level design and eco-efficient processing to replace petroleum-based hydrophobic polymers with renewable lignin derivatives.
2. We achieved waterborne spray coatings from palmitoylated lignin exhibiting durable hydrophobicity (WCA > 130°) and substantial mechanical reinforcement (wet tensile ↑ 400%). The process uses a bio-based acylating agent, avoids toxic reagents, and eliminates volatile organic solvents during coating formation.
3. Further optimization could replace pyridine with bio-derived, recyclable catalysts or green solvents, and extend the platform to reactive extrusion or continuous-flow synthesis for scalable, closed-loop lignin functionalization and coating production.

1. Introduction

The growing demand for sustainable alternatives to petroleum-derived polymers has intensified interest in renewable feedstocks, particularly plant biomass.[1] Among these, technical lignins are especially attractive as replacements for aromatic polymers due to their abundance as byproducts of pulping and biorefinery operations.[2,3] Despite their structural complexity and heterogeneity, lignins possess a high carbon content, diverse functional groups, and inherent UV stability, making them strong candidates for advanced material applications.[4–6] However, the relatively hydrophilic nature of technical lignins, arising mainly from the high density of hydroxyl groups, limits

[a]*Bioproducts Institute, University of British Columbia, 2385 East Mall, Vancouver, V6T 1Z3, Canada. E-mail: kwang.kim@ubc.ca, Orlando.rojas@ubc.ca*
[b]*Department of Wood Science, University of British Columbia, 2424 Main Mall, Vancouver, V6T 1Z4, Canada*
[c]*Department of Chemical and Biological Engineering, University of British Columbia, 2360 East Mall, Vancouver, V6T 1Z3, Canada*
[d]*One Packaging R&D Centre, Unilever, Bromborough Road, Bebington, Wirral, CH63 3JW, UK*
[e]*Department of Chemistry, University of British Columbia, 2036 Main Mall, Vancouver, V6T 1Z1, Canada*
†These authors contributed equally to this work.

their direct utility in applications requiring water repellency, such as hydrophobic surface coatings.[7–9]

Paper products, although renewable and biodegradable, are intrinsically hydrophilic and porous, which results in rapid water uptake and a pronounced loss of strength when exposed to moisture.[10] These limitations restrict their use in applications such as packaging, labeling, and disposable products where water resistance and durability are critical. With the rapid growth of the paper-based packaging sector, enhancing the water resistance of paper materials has become increasingly important.[11] To address these challenges, hydrophobic finishes are commonly applied to paper surfaces to impart water repellency, improve barrier performance, and enhance wet mechanical strength.[12,13] The development of bio-based and sustainable coating systems is therefore essential to reduce reliance on petroleum-derived polymers such as polyethylene (PE), polyethylene terephthalate (PET), polybutylene terephthalate (PBT), polyvinyl alcohol (PVOH), among other commonly used film-forming polymers.[14] A variety of coating methods have been explored for modifying paper, including dip coating, bar coating, knife coating, and spray coating.[15] Among these methods, spray coating offers several advantages, such as simplicity, scalability, and compatibility with a wide range of solvents. It can deposit thin, uniform, and controllable layers without saturating the porous paper structure, and it is already widely used in industrial coatings, paints, and graphic arts.[15]

To valorize lignin as a hydrophobic coating while addressing its inherent hydrophilicity, chemical modification *via* esterification has emerged as a promising strategy to tailor its physicochemical properties. Among the various acylation reagents, long-chain fatty acid anhydrides represent a renewable and effective option for imparting hydrophobicity while maintaining lignin's biobased character.[16,17] In particular, palmitic anhydride, a derivative of the naturally abundant and inexpensive palmitic acid, is especially attractive, as it enables the introduction of long alkyl chains that markedly reduce the surface energy of technical lignins.[18]

In addition to chemical modification, structuring lignin into colloidal lignin particles (CLPs) broadens its processability and enhances its functionality.[3,19] CLPs can be prepared through solvent shifting or other techniques, producing spherical particles with high colloidal stability and tunable surface chemistry.[19] Their particulate morphology offers unique advantages for coating applications, including improved film uniformity, controlled porosity, and enhanced barrier properties.[20] When combined with hydrophobic modification, CLPs present a versatile platform for developing sustainable water-repellency.[16] However, despite advances in lignin modification and particle formation, relatively few studies have linked molecular-level hydrophobicity to practical coating performance, adhesion, and reinforcement of paper substrates. Since adhesion and durability are critical requirements for most applications, in this study, lignin was chemically modified with palmitic anhydride and applied either directly as an acetone-based spray coating or, after conversion into hydrophobic colloidal particles, as a waterborne spray on paper substrates. The modification was hypothesized to enhance the water resistance of lignin by masking hydrophilic hydroxyl groups and introducing hydrophobic alkyl chains. Our findings demonstrate that fatty-acid-modified lignin, particularly when structured into particle-based coatings, offers a robust pathway to replace petroleum-derived hydrophobic coatings. This work establishes a platform for advancing sustainable, high-performance surface treatments.

2. Materials and methods

2.1. Materials

Softwood Kraft lignin (Amallin™ LPH) was provided by West Fraser Timber Co. Ltd (Canada). Palmitic anhydride, pyridine, acetone and 2-hydroxyethyl cellulose (HEC, average M_w ~380 000) were purchased from Millipore Sigma (Canada). Filter paper (Fisherbrand) was purchased from Fisher Scientific (Canada).

2.2. Palmitoylation of lignin

Palmitoylated lignin (p-lignin) was prepared by first washing 15 g of low-pH kraft lignin with 800 mL of deionized (DI) water under constant stirring for 24 h to remove impurity such as inorganic salts. The washed lignin was collected by vacuum filtration and oven-dried at 80 °C. Esterification was carried out by adding 2 g of washed kraft lignin and 5 g of palmitic anhydride into 50 mL of pyridine, followed by stirring in an oil bath at 60 °C for 3 h. Meanwhile, 800 mL of DI water was chilled in a refrigerator. After the reaction, the mixture was transferred dropwise into the chilled DI water while stirring. The suspension was separated into 45 mL Falcon tubes and centrifuged at 4000 rpm for 5 min. The supernatant was discarded, and the pellet was redispersed in 30 mL DI water and 10 mL ethanol, vortexed until homogeneous, and centrifuged again at the same settings. Washing was repeated until no white impurities were visible. Ethanol was removed by two additional washes with DI water only, and the final product was dried in a vacuum dryer for 12 h to obtain p-lignin.

2.3. Lignin coatings

Two sprayable coating formulations were prepared. For the acetone-based spray, 0.2 g of p-lignin was dissolved in 10 mL acetone and vortexed until fully dissolved (0.2% w/v concentration). For the waterborne spray, 0.5 g of p-lignin was dissolved in 10 mL acetone, followed by the addition of 25 mL DI water under stirring. The mixture was left in a fume hood until the acetone was completely removed. The final concentration of purified waterborne p-lignin spray was approximately 1.1% (w/v). Hydroxyethyl cellulose (HEC) was added to reach concentrations of 0.4%, 0.6%, 0.8%, and 1.0% (w/v) based on the volume of the spray.

Spray coating was carried out on 55 mm Whatman filter papers using an airbrush connected with nitrogen. For the acetone-based spray, four sets of samples were prepared with

1–4 spray cycles (500 μL per spray), and filter papers were weighed before and after spraying to calculate lignin deposition. A version of these samples was also prepared by oven heating at 80 °C for 7 min after spraying. For the water-borne HEC sprays, samples were prepared at 0.4–1.0% HEC with three spray cycles each. The coated samples were air dried to evaporate the water. Additional samples at 0.4% HEC were prepared with 1–4 sprays to evaluate the effect of increasing lignin loading.

2.4. Chemical, thermal and surface characterizations

Fourier-transform infrared spectroscopy (FTIR) of dried lignin samples was conducted in ATR mode using Bruker Invenio-S FTIR Spectrometer. Phosphorus-31 nuclear magnetic resonance (^{31}P NMR) analysis of lignin samples was performed on a Bruker Avance 400 MHz spectrometer equipped with a BBO probe with Z gradients. The resonance frequency for ^{31}P was 162.02254 MHz. The pulse program zgig was used, with a relaxation delay (d1) of 10 s and an acquisition time of 0.8 s. Spectra were collected over a chemical shift range of 190–90 ppm, with a total of 400 scans acquired. The sample preparation for ^{31}P NMR was performed following a method described by Fang *et al.*[6]

The thermal degradation characteristics of the lignin samples were determined by thermogravimetric analysis (TGA) using a TA instrument Q500 (New Castle, USA). The samples were heated to 110 °C and held isothermally for 10 min to remove residual moisture, then heated to 900 °C at 20 °C min^{-1}, followed by a 20 min isothermal hold at 900 °C.

Glass transition temperature (T_g) of lignin samples was determined by differential scanning calorimetry (DSC) using a TA Q1000 (TA Corporation, USA). DSC testing was conducted in three cycles: the first cycle heated the samples to 200 °C and the second cycle cooled to 40 °C to eliminate moisture, while the third cycle reheated them to 250 °C to determine the glass transition temperature.

The hydrophobicity of lignin samples was evaluated using water contact angle (WCA) measurements with a Theta Flex 300 pulsating drop tensiometer, and by dynamic vapor sorption (DVS) analysis with a DVS instrument from Surface Measurement Systems Ltd (USA). For DVS, approximately 10 mg of lignin powders were oven dried and carefully weighted prior to the measurement. For WCA measurements, lignin coatings on silica plates (2 × 2 cm) were prepared by spin-coating 200 μL of lignin solution (Kraft lignin in a 3 : 1 acetone–water mixture, and p-lignin in pure acetone), applied in five successive layers (total volume: 1 mL). A 5 μL water droplet was then placed on each coated plate, and its shape and volume were recorded for 60 s at 1.4 fps.

2.5. Molecular dynamics simulations

Atomic configurations of Kraft lignin and p-lignin were constructed using CHARMM-GUI and simulated in NAMD with the CHARMM General Force Field and TIP3P water model. Initial systems were generated with Packmol and equilibrated in the NPT ensemble with Langevin dynamics. Hydration free energies were calculated using the WtM–λABF method and binding free energies with the Ga–WtM–eABF method following GaMD pre-sampling. All simulations employed PME electrostatics, cutoff-based nonbonded interactions, and bond constraints. Free energy calculations were performed in duplicate, and structural and hydrogen-bond analyses were carried out using VMD and MD analysis. Detailed simulation methods are provided in the SI.

2.6. Lignin suspensions

The particle size and zeta potential of p-lignin particles were analyzed by a Zetasizer Nano-ZS (Malvern). The p-lignin suspension was diluted to 0.01 wt% prior to analysis. The viscosity of p-lignin suspensions was measured using Rheometer (MCR 302e, Anton Paar GmbH) equipped with double-gap measuring system. Test was performed within the shear rate range of 1–100 s^{-1} at 25 °C.

2.7. Lignin morphology and coatings (wettability roughness and adhesion)

SEM of p-lignin particles and the surface of control and coated filter papers were conducted using Zeiss X 350 SEM. For p-lignin particles, the suspension was diluted to 0.01% and air-dried on a silica wafer. All samples were sputter-coated with gold prior to imaging analysis. The confocal microscopy of control and coated filter papers was conducted using Leica STELLARIS 5 confocal microscope at 10 times magnification. Confocal imaging was performed using a 405 nm excitation wavelength, with emission signals detected across the 425–600 nm range, following the method by Wightman *et al.*[21]

The surface roughness of filter papers was analyzed with a Wyko NT1100 surface profiler (VSI mode, 20× objective, 1.0× FOV, 3× scan speed). Average roughness values were obtained from three measurements at different locations on each sample. Surfaces of uncoated filter paper, acetone-coated paper, and water-borne coated paper were compared. Water contact angle of filter papers was measured using a Theta Flex 300 pulsating drop tensiometer. Each filter paper sample was measured in triplicate at different positions. Adhesion of coatings was assessed using a tape test with 18 mm 3 M tape (Cat. 810D), which was applied to the coated surfaces and peeled to evaluate coating attachability.

2.8. Tensile tests of coated papers

The dry and wet tensile strength of filter paper samples were measured using a TMI Büchel Horizontal Tensile Tester (Model 84-56). Whatman filter papers (150 mm diameter) were cut into strips of 13 × 1.5 cm. Paper strips were coated following the waterborne coating procedure described above, three times on each side. Dry strength was tested directly, while wet strength was evaluated by submerging the mid-section of each strip in DI water for 30 s prior to testing. For each condition, three replicates were tested.

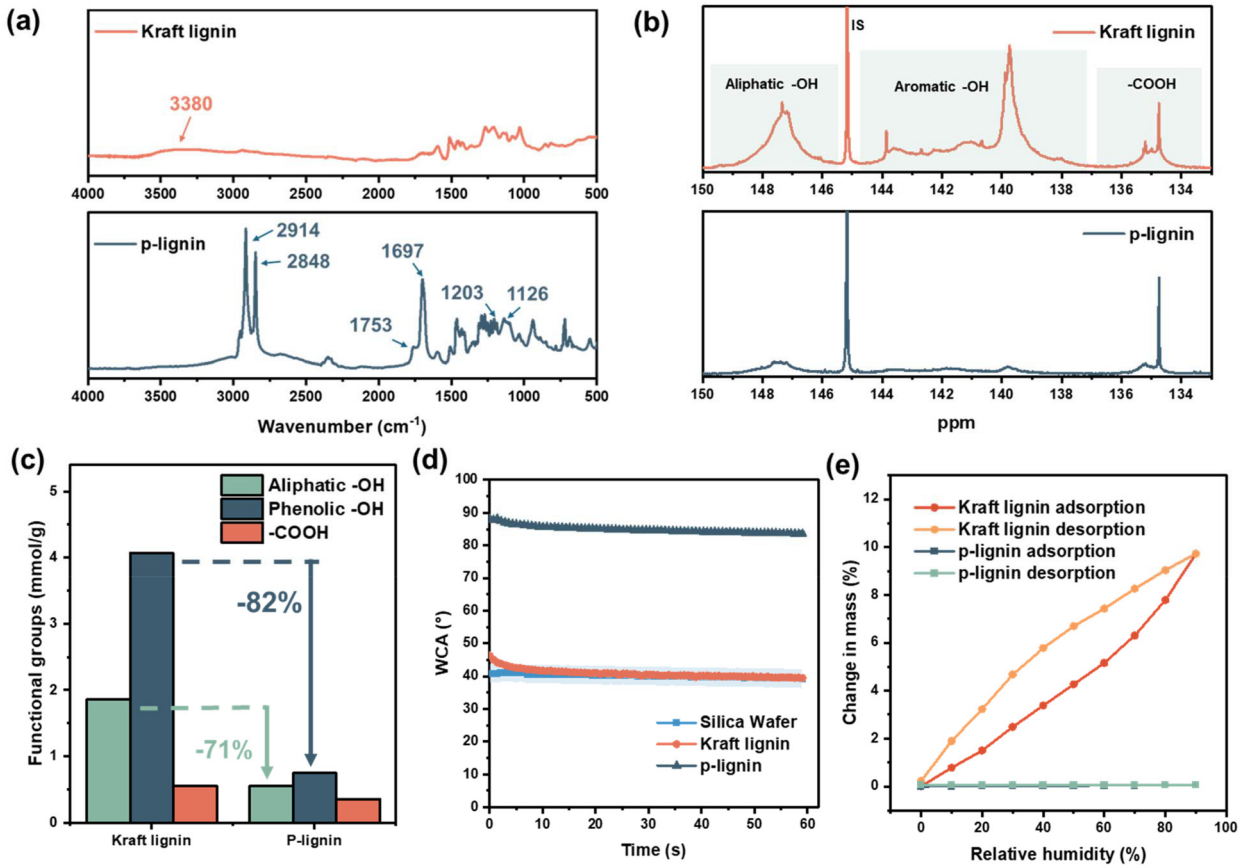

Fig. 1 Characterization of kraft lignin and p-lignin: (a) FTIR and (b) ^{31}P NMR spectra. (c) Summary of functional group content (NMR). (d) Water contact angle of silica wafer (support), kraft lignin and p-lignin spin-coated on silica wafers. (e) DVS adsorption/desorption isotherms of kraft lignin and p-lignin.

3. Results and discussion

3.1. Increasing hydrophobicity of kraft lignin *via* palmitoylation

The successful modification of Kraft lignin into p-lignin was initially evaluated through the characterization of its functional groups using FTIR spectroscopy (Fig. 1a) and quantitative ^{31}P NMR analysis (Fig. 1b and c). The FTIR spectra provided clear evidence of chemical modification, as a notable reduction in the broad O–H stretching band at 3380 cm^{-1} indicated the consumption of hydroxyl groups, while the emergence of new absorption bands at 1753 and 1697 cm^{-1} was attributed to the C=O stretching vibrations of aliphatic and aromatic esters, respectively. Moreover, distinct bands at 2914 and 2848 cm^{-1}, corresponding to the asymmetric and symmetric C–H stretching of aliphatic chains, confirmed the incorporation of long-chain palmitic moieties into the lignin backbone through ester linkages. Complementary insights were obtained from ^{31}P NMR, which allowed quantitative determination of hydroxyl group substitution. The analysis showed 71% and 82% conversion of aliphatic and phenolic hydroxyls, respectively, into esterified palmitic groups (Fig. 1c). Together, these results demonstrate a high degree of substitution and provide strong evidence for the effective esterification of Kraft lignin with palmitic groups.

It is anticipated that the long hydrophobic chains resulted from palmitoylation of hydroxyl groups would disrupt the extensive inter- and intramolecular hydrogen bonding network within lignin, thereby lowering its glass transition temperature and diminishing its thermal stability, as shown in previous work by Liu *et al.*[17] Since thermal behavior is critical for defining the processing window of lignin, these effects were systematically evaluated by DSC and TGA. DSC analysis confirmed that incorporation of palmitic groups markedly decreased the glass transition temperature (T_g) of lignin, from 170 °C to 61 °C (Table 1, Fig. S1a). TGA further revealed that thermal degradation shifted to lower temperatures due to the incorporation of palmitic groups, as evidenced by a lower $T_{d\ 5\%}$ (temp-

Table 1 Thermal properties of starting Kraft lignin and p-lignin

Sample	T_g (°C)	Temperature at 5% weight loss (°C)	Char content at 800 °C (%)
Kraft lignin	170	265	37
P-lignin	61	188	13

erature at 5% weight loss), a distinct weight loss event near 250 °C associated with degradation of the palmitic chains, and a decreased char yield at 800 °C due to lower content of phenolics (Table 1, Fig. S1b). These results validate the hypothesis that palmitoylation fundamentally alters the thermal characteristics of lignin, which has important implications for its processability and application in thermally sensitive systems.

The water contact angle (WCA) increased substantially from approximately 40° for Kraft lignin to nearly 90° for palmitoylated lignin (p-lignin), indicating that the introduction of long aliphatic chains effectively reduced surface wettability (Fig. 1d). The enhanced hydrophobicity of p-lignin was further validated by dynamic vapor sorption (DVS) analysis. While Kraft lignin readily absorbed moisture, showing a weight gain of up to 10% at 90% relative humidity, p-lignin exhibited minimal weight fluctuation and remained nearly constant across the entire sorption–desorption cycle (Fig. 1e). These findings confirm that substitution of hydroxyl groups with palmitic moieties imparts a durable hydrophobic character to the lignin.

The experimental results were complemented by molecular dynamics simulations using model compounds of Kraft lignin and p-lignin (Fig. 2a), enabling the evaluation of their hydration and binding free energies. Hydration free energy ($\Delta G_{hydration}$) quantifies molecular hydrophobicity as the free energy change associated with transfer from the gas phase to water, while binding free energy characterizes the tendency of hydrophobic groups or surfaces to associate in aqueous environments, a key manifestation of the hydrophobic effect.[22,23] The free energy results derived from alchemical

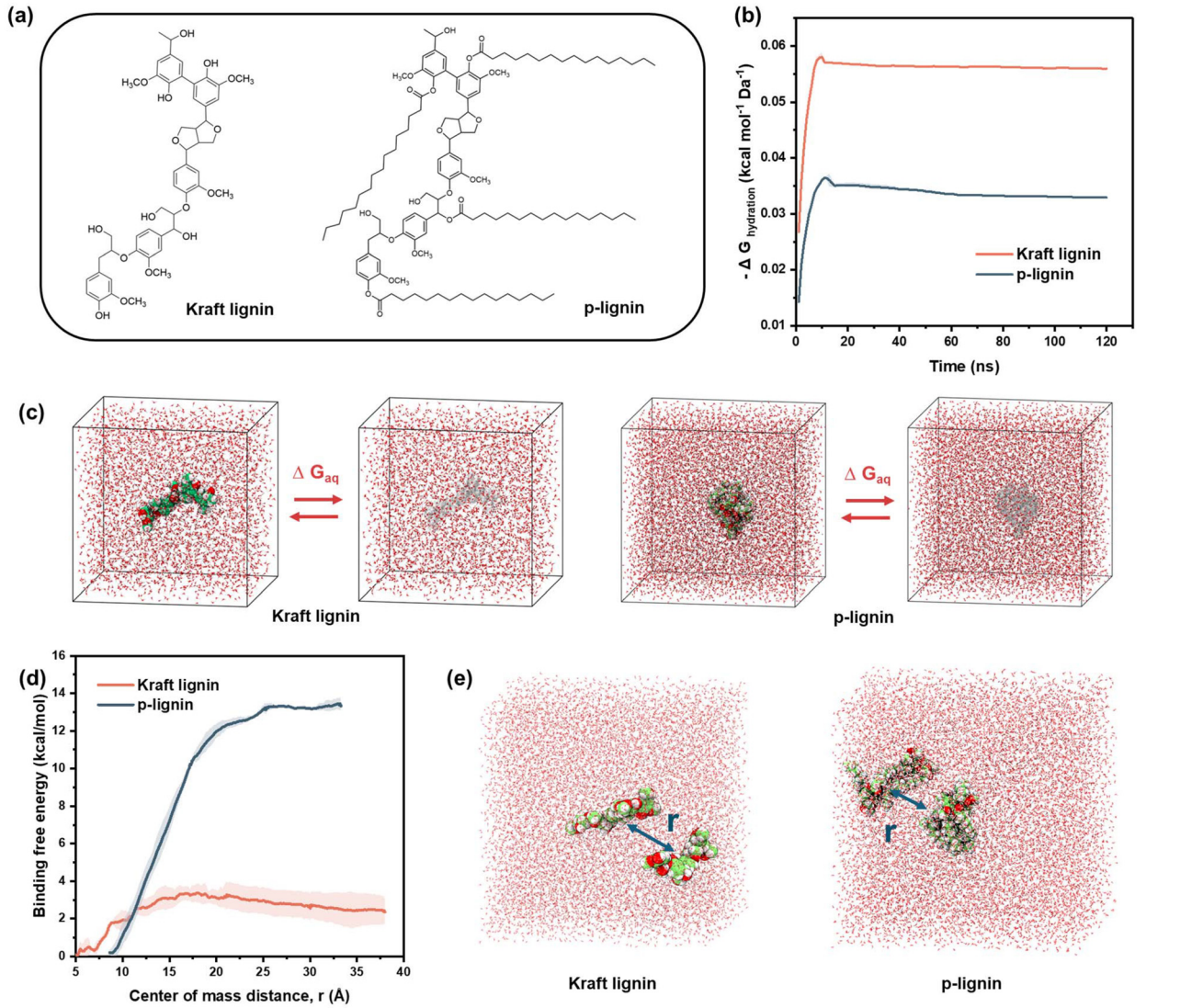

Fig. 2 Molecular dynamics simulation: (a) representative model molecules of Kraft lignin and p-lignin. (b) Time evolution of the hydration free energy ($-\Delta G_{hydration}$) and (c) atomistic models used for hydration free-energy calculations of Kraft lignin and p-lignin. (d) Binding free energy as a function of the center-of-mass separation between two lignin molecules for Kraft lignin and p-lignin, and (e) atomistic configurations used for binding free-energy calculations of Kraft lignin and p-lignin.

transformations revealed the hydration free energies of Kraft lignin and p-lignin surfaces in water, normalized by surface area (Fig. 2b and c). For Kraft lignin, the normalized hydration free energy (ΔG_{hk}) was −0.059 kcal mol^{-1} Å^{-2}, whereas for p-lignin it was less negative (ΔG_{hp} = −0.030 kcal mol^{-1} Å^{-2}), suggesting weaker interactions with water and thus greater hydrophobicity of p-lignin. Furthermore, the binding free energy of p-lignin (ΔG_{bp}) was approximately −13.44 kcal mol^{-1} at the convergence position between two p-lignin entities (r = 33 Å), nearly fivefold greater in magnitude than that of Kraft lignin (ΔG_{bk} = −2.46 kcal mol^{-1} at r = 37 Å) (Fig. 2d and e). The resulting difference in binding free energy ($\Delta G_{bk} - \Delta G_{bp} \approx 10.98$ kcal mol^{-1}) corresponds to ~18 RT (RT ≈ 0.6 kcal mol^{-1} at 300 K), which translates into an ~8.9×10^7-fold increase in the equilibrium constant comparison ($\frac{k_{\text{p-lignin}}}{k_{\text{kraft-lignin}}} = e^{-\frac{\Delta G_{bk} - \Delta G_{bp}}{RT}}$), signifying a dramatically stronger propensity to aggregate for p-lignin in aqueous environments compared with Kraft lignin.

3.2. Hydrophobic coatings from p-lignin

An initial trial in the current study using an acetone-based p-lignin coating significantly enhanced the hydrophobicity of filter paper, achieving a water contact angle (WCA) over 140° with just 0.2 mg cm^{-2} loading, and exceeding 150° with increased deposition (Fig. S2). However, the coating lacked strong adhesion, as shown by a tape test (Fig. S3). Oven curing, previously reported to promote the abrasion resistance of lignin coating on wood surface,[24] was conducted at 80 °C and improved adhesion by promoting polymer binding, though it slightly reduced WCA to ~130° (Fig. S2). Despite its effectiveness, the use of flammable acetone poses safety concerns for large-scale applications.[25] As a result, the study shifted focus toward developing a safer, waterborne p-lignin coating for improved practicality and commercial viability. This was achieved by producing negatively charged colloidal p-lignin particles with an average size of approximately 200 nm (Fig. 3a, Table S1) through dissolution in acetone followed by precipitation into water, forming stable suspensions. However, water-based spray coatings exhibited uneven deposition due to slow evaporation and the heterogeneous paper surface, leading to non-uniform wetting, penetration, and fluid redistribution, which caused irregular coating patterns (Fig. S4).

To address the limitations of waterborne paper coating, hydroxyethyl cellulose (HEC), a commonly used thickening agent in the coating industry, was incorporated into the p-lignin suspension.[26] It was recognized that the use of HEC should be minimized, as it would compromise the hydrophobicity of the coating given its hydrophilic nature. In this study, HEC loadings of 0.4%, 0.6%, 0.8%, and 1% were tested, and the resulting increase in suspension viscosity, confirmed by shear viscosity measurements (Fig. 3b), facilitated successful application of p-lignin onto filter paper. The addition of HEC regulated droplet spreading during spraying and drying, leading to more uniform and consistent coating layers across the paper surface (Fig. S4). At lower HEC loadings, the viscosity was insufficient to achieve satisfactory coating performance, with 0.4% identified as the minimum effective concentration .

To investigate the surface morphology of p-lignin coatings, SEM was employed on starting filter paper and coated with

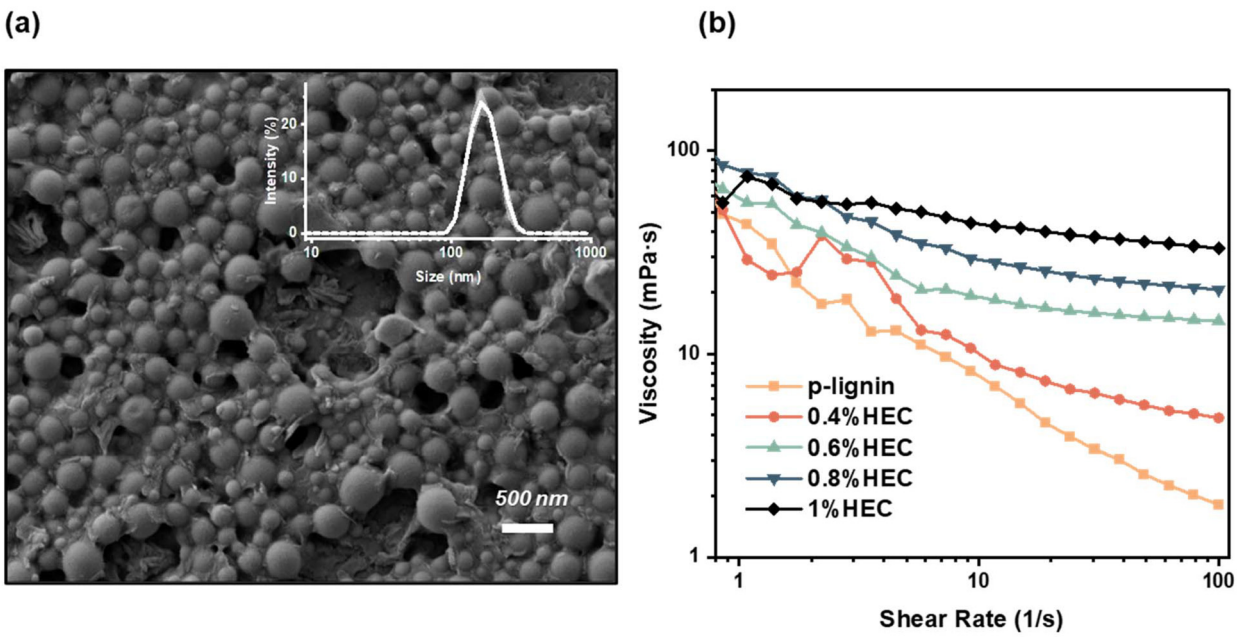

Fig. 3 (a) SEM images and particle size distribution of colloidal p-lignin particles, (b) shear viscosity of p-lignin suspension with and without HEC supplementation.

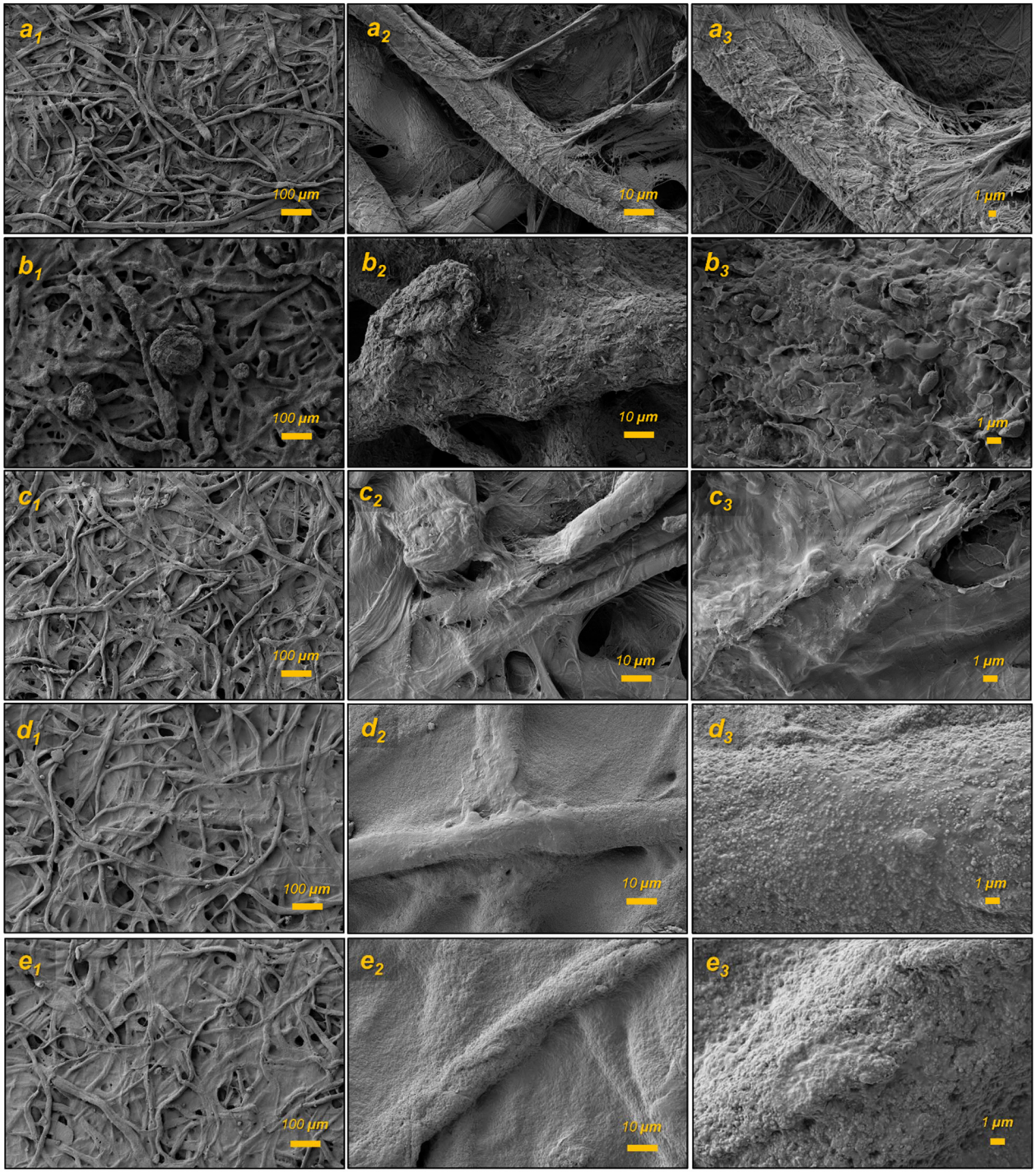

Fig. 4 SEM images of the surface of filter paper: (a) uncoated, (b and c) acetone-based p-lignin (b: no curing, c: oven-cured), and (d and e) waterborne p-lignin (d: 0.4% HEC, e: 1% HEC).

acetone and waterborne p-lignin coating supplemented with 0.4% and 1% HEC (Fig. 4). Compared to the starting filter paper, the surface of the acetone-coated paper was rough, as p-lignin formed large particles upon acetone evaporation (Fig. 4a and b). Since the oven curing temperature was higher than the T_g of p-lignin, the lignin likely migrated across the surface during curing, resulting in a more uniform distribution and fewer visible particles (Fig. 4c). In contrast, the waterborne p-lignin coating produced a more uniform distribution and a smoother surface (Fig. 4d and e), as also indicated by surface roughness measurements, which showed lower R_a and R_q values for filter paper coated with waterborne

p-lignin compared to acetone-based p-lignin (Fig. S5). At higher SEM magnification, dried spherical lignin nanoparticles were observed on the fiber surfaces (Fig. 4d$_3$ and e$_3$).

Subsequently, confocal microscopy was employed to examine the distribution of p-lignin on the coated filter papers. By taking advantage of the intrinsic autofluorescence of lignin,[21] lignin could be visualized without additional staining, while the control filter paper (cellulose only) exhibited no detectable signal (Fig. 5). Both acetone-based and waterborne coatings produced observable lignin coverage, but the water-

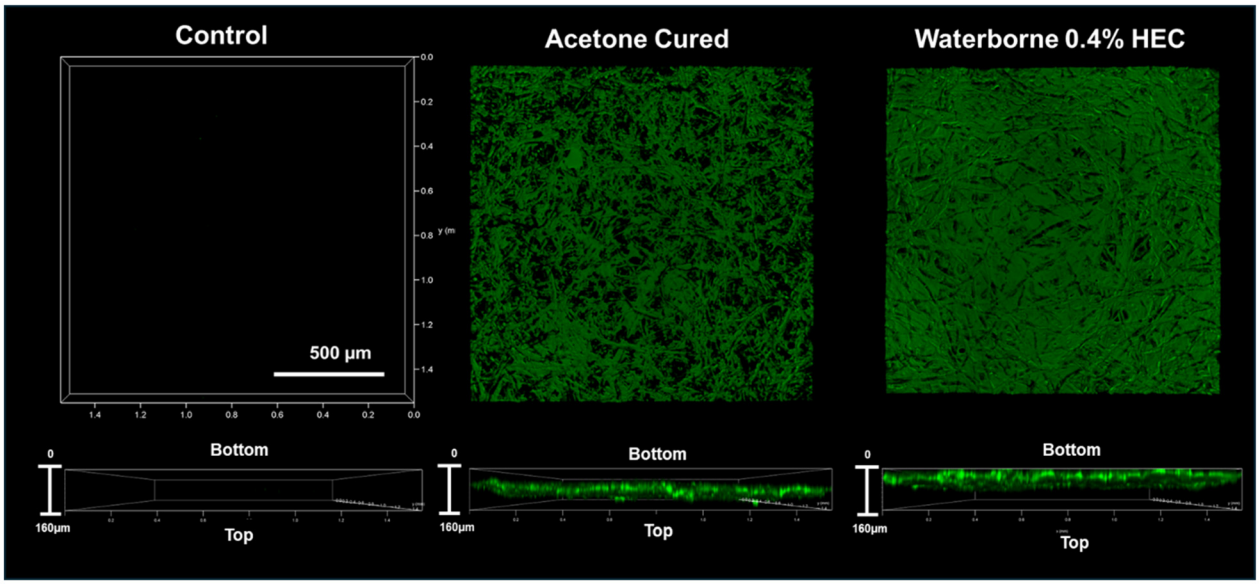

Fig. 5 3D confocal microscopy of filter paper before and after three sprays of p-lignin coatings: acetone-based (cured) and waterborne (with 0.4% HEC).

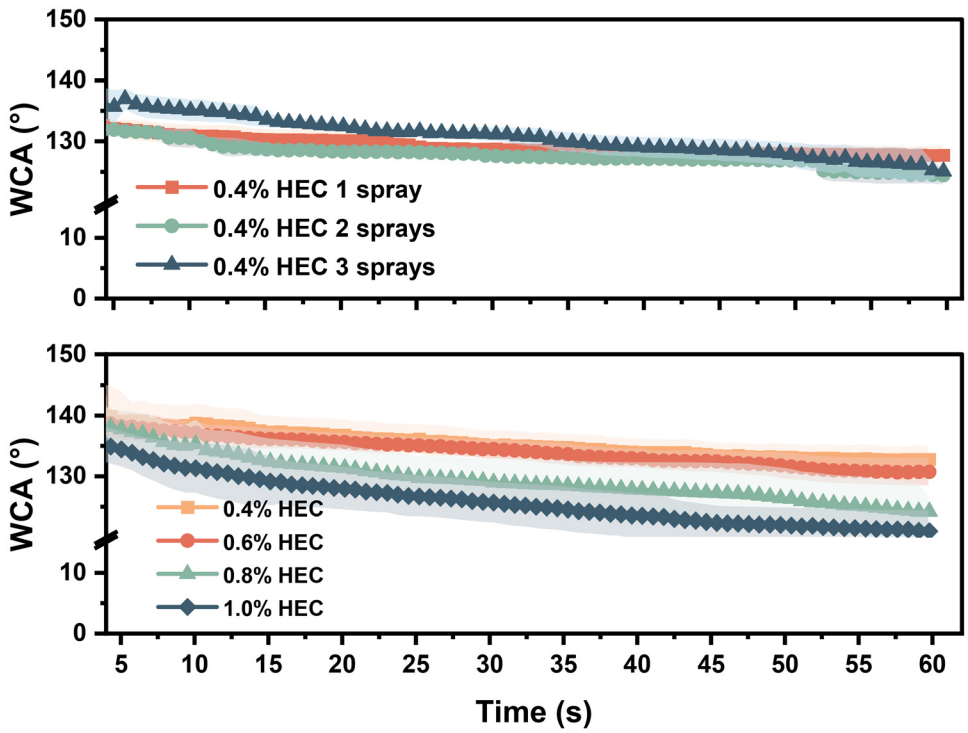

Fig. 6 Water contact angle (WCA) of waterborne p-lignin spray over 60 s: effect of spray cycles at 0.4% HEC (top) and effect of HEC loading at three spray cycles (bottom).

borne formulation resulted in a more continuous and extensive surface distribution compared to the acetone coating. Three-dimensional confocal imaging, with optical sectioning up to 100 μm in depth, further revealed that the waterborne coating promoted deeper penetration of p-lignin into the fiber network (Fig. 5). This enhanced penetration is likely due to the slower evaporation rate of water, which allows p-lignin to diffuse into the porous structure, whereas the rapid evaporation of acetone restricts lignin deposition mainly to the surface.

The subsequent WCA tests of the coated filter papers indicated that one spray of waterborne p-lignin coating with 0.4% HEC was able to achieve WCA of approximately 130°, which could be slightly increased by applying more layers of coatings (Fig. 6). At three sprays of waterborne coatings (approximately 0.6 mg lignin per cm^2), increasing HEC content led to a slight decrease in WCA, likely due to more hydrophilic nature of HEC (as filter paper coated with HEC showed no measurable WCA). Nonetheless, all coatings still exhibited WCA values greater than 120° that persisted for at least 1 min (Fig. 6), comparable to the acetone-based coating after curing (Fig. S2). This result was promising compared to the use of other bio-based polymers, such as modified chitosan, which has been reported to increase the water contact angle (WCA) of filter paper to 110–150° *via* water dip-coating,[27,28] and polyhydroxybutyrate (PHB), which achieved a WCA of 153° using dip-coating in chloroform.[29] Petroleum-based coatings can reach even higher hydrophobicity. For example, a study using low-density polyethylene (LDPE) to coat filter paper through dissolution in *o*-xylene and casting achieved a WCA of 158°, though this came at the expense of greater environmental impact.[30] In contrast, our approach offers advantages by employing a simple, waterborne spray-coating process. Since 0.4% HEC provided satisfactory coating performance, it was selected as the optimum loading. Notably, without the need for oven curing, the waterborne coating demonstrated strong adhesion to the filter paper, as confirmed by the tape adhesion test (Fig. S3).

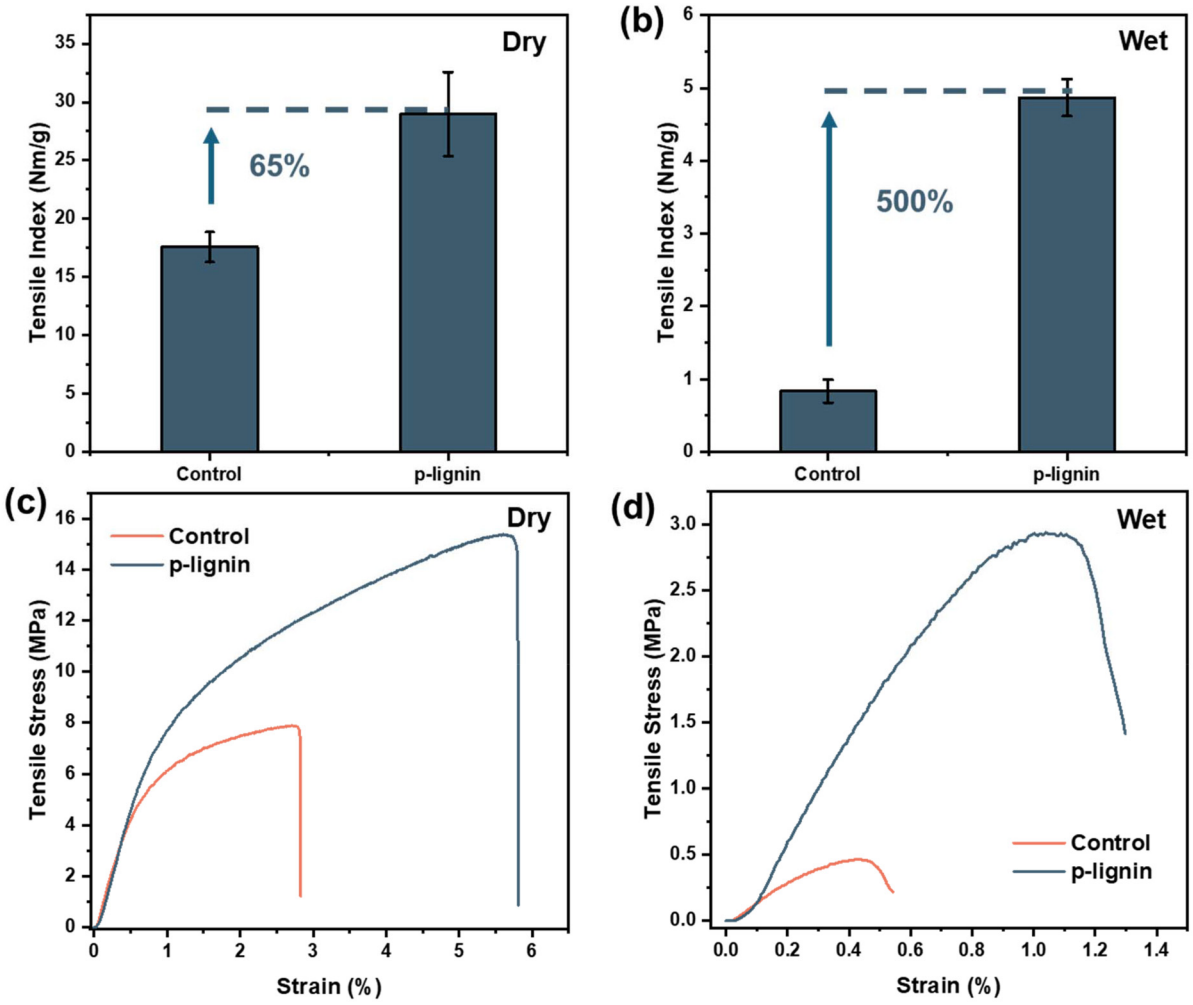

Fig. 7 Tensile indices (a and b) and representative stress–strain curves (c and d) of filter papers before (control) and after waterborne p-lignin coating. Panels a and c show dry strength, while panels b and d show wet strength.

3.3. Mechanical strength of coated paper

One of the primary applications of hydrophobic coatings on paper products is in packaging, where wet tensile strength is a critical performance parameter.[11] Given that the waterborne coating (*i.e.*, p-lignin with 0.4% HEC) produced more uniform and deeper deposition of p-lignin on the filter paper, this formulation was selected to evaluate its potential for enhancing wet tensile properties, by coating both sides of the filter paper for three cycles. It is important to note that the filter paper used in this study is known to contain inherent wet-strength additives, which enables it to exhibit measurable wet tensile strength as a control, in contrast to typical handsheets prepared from Kraft pulp.[31] Promisingly, the combination of p-lignin and HEC likely reinforced the fiber network, resulting in a substantial improvement even in dry tensile performance. Specifically, the dry tensile index increased by approximately 65%, from 18 to 29 N m g^{-1} (Fig. 7a), and the corresponding stress–strain curves indicated enhancements in both tensile strength and elongation (Fig. 7c). Regarding wet tensile strength, p-lignin coating produced a remarkable increase of almost 500%, from 0.8 to 4.9 N m g^{-1} (Fig. 7b), accompanied by improvements in both strength and strain as reflected in the stress–strain curves (Fig. 7d). These results indicate that the enhanced hydrophobicity imparted by the p-lignin coating substantially improves the durability of the paper under wet conditions. Furthermore, the simplicity and scalability of this coating strategy highlight its potential applicability across a wide range of paper substrates and grades, making it a promising approach for high-performance packaging applications.

4. Conclusions

This study demonstrated that esterification of softwood Kraft lignin with palmitic anhydride produced p-lignin with substantially enhanced hydrophobicity, as evidenced by water contact angle measurements, dynamic vapor sorption, and molecular dynamics simulations. Both acetone-based and waterborne p-lignin coatings achieved water contact angles above 130° sustained for over one minute, confirming durable water repellency. While the acetone-based coating required low-temperature curing (80 °C) to ensure adhesion, the waterborne formulation provided comparable hydrophobicity and adhesion, with the added advantage of deeper penetration into the paper matrix. In addition, p-lignin coatings markedly improved the wet strength of filter paper, highlighting their promise as scalable, bio-based alternatives for high-performance and sustainable packaging applications. Research may advance this work by extending p-lignin coatings to a wider range of substrate systems and refining process efficiency, alongside integrated assessments of biodegradability, carbon footprint, and techno-economic feasibility, as well as expanded mechanical characterization of the coating-substrate interactions to accelerate the translation of the technology.

Author contributions

JW: conceptualization, methodology, investigation, writing – original draft preparation. NH: methodology, investigation. DB-R: methodology, investigation. ZW: methodology, investigation. MY: methodology, investigation. XS: methodology, investigation. YH: methodology, investigation. JB: methodology, investigation. OE: methodology, investigation, OJR: conceptualization, supervision, funding acquisition, writing – review & editing. KHK: conceptualization, supervision, funding acquisition, writing – review & editing. All authors approved the final manuscript.

Conflicts of interest

The authors declare that they have no known competing financial interests.

Data availability

The authors confirm that the data supporting the findings of this study are available within the article and its supplementary information (SI). Supplementary information: DSC, TGA, WCA, surface roughness, photo of the treated papers products, and particle size. See DOI: https://doi.org/10.1039/d5gc05423k.

Acknowledgements

The authors would like to thank Unilever PLC for financial support and Dr Guang Gao from UBC Life Sciences Institute for his guidance with the confocal microscopy. This study is also supported by the Natural Sciences and Engineering Research Council of Canada Global Center for Sustainable Bioproducts program. O. J. R. and J. W. also acknoweledge the Canada Excellence Research Chair Program (CERC-2018-00006), Canada Foundation for Innovation (38623), Pacific Economic Development Canada (PacifiCan), and the British Columbia Ministry of Forest. We thank the support provided by the British Columbia Digital Research Infrastructure (DRI) Group; the Digital Research Alliance of Canada (alliancecan.ca) and the Advanced Research Computing at the University of British Columbia.

References

1 Y. Yu, J. Wu, X. Ren, A. Lau, H. Rezaei, M. Takada, X. Bi and S. Sokhansanj, *Renewable Sustainable Energy Rev.*, 2022, **154**, 111871.
2 J. Wu, R. P. Chandra, K. H. Kim, C. S. Kim, Y. Pu, A. J. Ragauskas and J. N. Saddler, *ACS Sustainable Chem. Eng.*, 2020, **8**, 5847–5855.

3 D. Barker-Rothschild, J. Chen, Z. Wan, S. Renneckar, I. Burgert, Y. Ding, Y. Lu and O. J. Rojas, *Chem. Soc. Rev.*, 2024, **54**, 623–652.
4 Q. Hua, Z. Huang, J. Gou, H. Zhang, I. Therrien, J. Wu, Y. Liang and S. Renneckar, *Chem. Eng. J.*, 2024, **499**, 156139.
5 Q. Hua, M. A. Karaaslan, Z. Huang, L. Fang, J. Wu, H. Zhang, Y. Ye, Y. Abdin and S. Renneckar, *Adv. Funct. Mater.*, 2025, **09131**, 1–13.
6 L. Fang, Q. Hua, J. Wu, Z. Huang, H. Zhang, Q. Yong, J. Saddler and S. Renneckar, *ACS Sustainable Chem. Eng.*, 2025, **13**, 14411–14424.
7 M. Farooq, Z. Tao, J. J. Valle-Delgado, M. H. Sipponen, M. Morits and M. Österberg, *Langmuir*, 2020, **36**, 15592–15602.
8 J. Liu, J. Wu, Y. Lu, H. Zhang, Q. Hua, R. Bi, O. Rojas, S. Renneckar, S. Fan, Z. Xiao and J. Saddler, *Bioresour. Technol.*, 2023, **367**, 128276.
9 M. Borrega, S. Päärnilä, L. G. Greca, A. S. Jääskeläinen, T. Ohra-Aho, O. J. Rojas and T. Tamminen, *Langmuir*, 2020, **36**, 9675–9684.
10 J. Wu, N. H. L. Ting, S. Chen, T. Zou, Q. Hua, Y. Yuan, M. A. Karaaslan and S. Renneckar, *Cellulose*, 2024, **31**, 7685–7696.
11 T. Lindström, L. Wågberg and T. Larsson, in *13th fundamental research symposium*, The Pulp and Paper Fundamental Research Society Cambridge, UK, 2005, vol. 32, pp. 457–562.
12 H. Huang, L. Mao, W. Wang, Z. Li and C. Qin, *Int. J. Biol. Macromol.*, 2023, **236**, 123630.
13 J. Song and O. J. Rojas, *Nord. Pulp Pap. Res. J.*, 2013, **28**, 216–238.
14 A. Adibi, B. M. Trinh and T. H. Mekonnen, *Prog. Org. Coat.*, 2023, **181**, 107566.
15 P. K. Kunam, D. Ramakanth, K. Akhila and K. K. Gaikwad, *Biomass Convers. Biorefin.*, 2024, **14**, 12637–12652.
16 M. Andersson, I. V. Pylypchuk, A. E. Alexakis, L. Y. Liu and M. H. Sipponen, *ACS Appl. Mater. Interfaces*, 2025, **17**, 1931–1941.
17 L. Y. Liu, Q. Hua and S. Renneckar, *Green Chem.*, 2019, **21**, 3682–3692.
18 M. Kim, Y. A. Lee, J. Wu, H. Kim, J. K. Ko, M. W. Moon, C. G. Yoo, K. Jeong and K. H. Kim, *ACS Appl. Polym. Mater.*, 2025, **7**, 503–511.
19 M. Österberg, M. H. Sipponen, B. D. Mattos and O. J. Rojas, *Green Chem.*, 2020, **22**, 2712–2733.
20 B. Las-Casas, J. Wu, O. J. Rojas and V. Arantes, *Int. J. Biol. Macromol.*, 2025, 147013.
21 R. Wightman, M. Busse-Wicher and P. Dupree, *Micron*, 2019, **126**, 102733.
22 H. Chen, H. Fu, C. Chipot, X. Shao and W. Cai, *J. Chem. Theory Comput.*, 2021, **17**, 3886–3894.
23 M. Zhou, X. Shao, W. Cai, C. Chipot and H. Fu, *J. Phys. Chem. Lett.*, 2025, **16**, 4419–4427.
24 K. A. Henn, N. Forsman, T. Zou and M. Österberg, *ACS Appl. Mater. Interfaces*, 2021, **13**, 34793–34806.
25 H. İskender, *Acad. Perspect. Procedia*, 2020, **3**, 927–934.
26 S. S. Gwebu and H. Chiririwa, *Int. J. Appl. Chem.*, 2017, **13**, 1–13.
27 X. Li, Z. Yu, Q. Chen, S. Yang, F. Li and Y. Yang, *Mater. Technol.*, 2018, 1–11.
28 N. Bordenave, S. Grelier and V. Coma, *Biomacromolecules*, 2010, **11**, 88–96.
29 C. G. Obeso, M. P. Sousa, W. Song, M. A. Rodriguez-pérez, B. Bhushan and J. F. Mano, *Colloids Surf., A*, 2013, **416**, 51–55.
30 M. Satapathy, P. Varshney, D. Nanda, A. Panda, S. S. Mohapatra and A. Kumar, *Cellulose*, 2017, **24**, 4405–4418.
31 X. Zhou, Y. Fu, L. Chen, R. Wang, X. Wang, Y. Miao, X. Ji, H. Bian and H. Dai, *Carbohydr. Polym.*, 2020, **248**, 116791.